Journal of Molecular Liquids, 47 (1990) 139–160
Elsevier Science Publishers B.V., Amsterdam

Monte Carlo Simulation Studies of the Solvation of Ions. 3. The non intramolecularly H-bonded Form of Glycine Zwitterion.

Giuliano Alagona and Caterina Ghio

Istituto di Chimica Quantistica ed Energetica Molecolare del C.N.R.
Via Risorgimento 35, I-56126 Pisa (Italy)

(Received 22 January 1990)

Abstract

The stability and the characteristics of the water solution of the non intramolecularly H-bonded (φ=60°) form of glycine zwitterion were studied with a Monte Carlo simulation in the N,P,T ensemble, using TIP4P potentials for water and analogous transferable potentials for glycine. The results were compared with those from previous simulations of glycine (φ=0°) and of its component ions. The analysis of the solution shows the presence of the same four types of water already found: (1) bulk waters; (2) hydrophobically bound waters near the CH_2 group; waters tightly bound (3) to the polar oxygens and (4) to the polar hydrogens. The energetics of the solution process is more favourable for the φ=60° form than for the φ=0° one, as far as the enthalpic term is concerned, by 2.6 kcal/mol, due to the compensation between the presence of an additional H-bond with water, coupled with a slightly smaller disruption of the solvent, and less favourable individual H-bonds on the average. Conversely, a considerable increase in the partial molar volume is detected. The in vacuo energy difference (including Hartree-Fock and thermal energies) between the two conformers at the 6-31G* level favours the φ=0° form with respect to the φ=60° one by about 5 kcal/mol, thus the former should be the most likely to be found in solution as well.

Introduction

Some authors which study solute-water interactions with the "super-molecule" approach, or with the solvent represented as a continuous

0167-7322/90/$03.50

medium, prefer to disregard solute structures involving intramolecular H-bonds, in that they consider it extremely difficult that these bonds are broken upon interactions with a few water molecules or with a continuum [1-2], as conversely occurs in real solutions, where extended configurations of oligopeptides prevail, even though less flexible groups, showing marked conformational preferences [3], are introduced [4]. To evaluate the soundness of this approximation in the case of very small solutes as well, and to determine to what extent the presence of the intramolecular H-bond had affected the structure and the energetics of the solution in our previous simulation of glycine zwitterion [5] (hereafter referred to as I), we decided to carry out the Monte Carlo simulation of the conformer with a torsional angle of 60°, hereafter referred to as II (see the schematic representation reported in Fig. 1), that in vacuo is less stable than I [6]. These simulations are then compared one to the other and to the simulations of the individual ions, $CH_3NH_3^+$ and CH_3COO^- [7], that made use as far as possible of the same parameters. A fairly extensive comparison of our results with those of

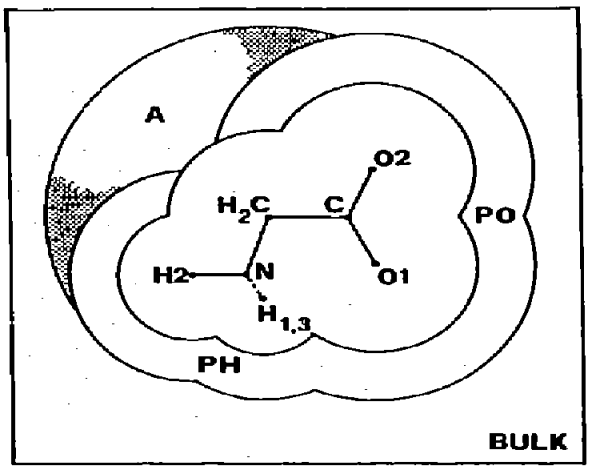

Fig. 1. Schematic representation of the solute conformation, of the solution specimen (a box with an average edge of 18.81 Å) and of the different solvation regions considered (A=apolar, PH=polar H, PO=polar O, bulk all the rest). The blank area surrounding the solute atoms stands for their excluded volume.

previous simulations of glycine zwitterion [8,9], using different potentials and ensembles, is reported in Ref. 5.

Methods

The simulation was carried out in the N,P,T ensemble (at 25°C and 1 atm) on a sample of 216 waters plus one molecule of the solute, using periodic boundary conditions with a non-bonded cutoff of 8.5 Å, in the Metropolis framework, supplemented with preferential sampling, on our Gould 3287/05.

Assuming pairwise additivity, the intermolecular potential between monomers m and n employed in the simulation is of the 12-6-1 type:

$$\varepsilon_{mn} = \sum_{i}^{\text{over m}} \sum_{j}^{\text{over n}} \left(\frac{q_i q_j e^2}{r_{ij}} + \frac{A_i A_j}{r_{ij}^{12}} - \frac{C_i C_j}{r_{ij}^{6}} \right)$$

Table 1. Parameters employed in the Monte Carlo simulation[a].

System	Atom type	$A^2 \times 10^{-3}$	C^2	q
	O	600	610	0
H_2O[b] - TIP4P	M	0	0	-1.04
	H	0	0	0.52
	$O^{\delta-}$	230.584	429.5	-0.745
	C	789.954	615.77	0.752
$H_3^+N\text{-}CH_2\text{-}COO^-$[c]	C2	7290	1825	0.270
	N	990.525	563	-0.663
	H	0	0	0.377

[a] Units: electrons for q; kcal-Å^{12}-mol^{-1} for A^2; kcal-Å^6-mol^{-1} for C^2.

[b] Experimental geometry (OH=0.9572 Å, <HOH=104.52°); M is located 0.15 Å away from O along the bisector of the HOH angle. Parameters from Ref. 10.

[c] Charges obtained by fitting the electrostatic potential produced by a 6-31G* wave function [11]; parameters from Ref. 12, except those of C2 [13]; geometric parameters: CO=1.25 Å, CC=1.53 Å, CN=1.48 Å, NH=1.03 Å, <OCO=125°, <HNH=109.47°, <NCC=109.47°, <HNC=109.47°.

For the sake of easier comparison the same procedure, the same parameters, and the same internal geometry of the solute (apart the φ=60° dihedral angle) as those used in the previous simulation [5] have been employed. The relevant parameters are reported in Table 1.

In order to analyze the structure of the solution we resorted to the partition of the first solvation layer already adopted in our previous simulations and, therefore, the first shell around glycine zwitterion was divided in three regions: A (apolar zone), PO (polar oxygen zone), PH (polar hydrogen zone), whose radii (derived from the minima of the relevant radial distribution functions) are exactly consistent with those employed for glycine I. These regions are also schematized in Fig. 1: the shaded regions represent the second solvation shell with respect to the polar first shell and, in our opinion, cannot be considered as belonging to the apolar hydration shell.

Results

Solute-solvent structural analysis

Radial distribution functions

We report in Fig. 2(a,b) the solute-solvent radial distribution functions, rdfs, (solid line), superimposed to the correspondent ones for glycine I (dashed line), recorded every step, scanning the space surrounding each solute atom with a Δr=0.055 Å. In the same plot (right scale) the relevant running coordination numbers are displayed (solid line) in comparison to those of glycine I (dashed line). Such a pictorial representation is more effective, despite the crowded aspect of the plots, and makes it easier to describe analogies and differences between the curves for the two conformers. For this reason we maintain the same choice as previously of rdfs displayed, keeping apart the radial distribution functions for the solute atoms (H1 and O1) that were involved in the intramolecular H-bond, to allow

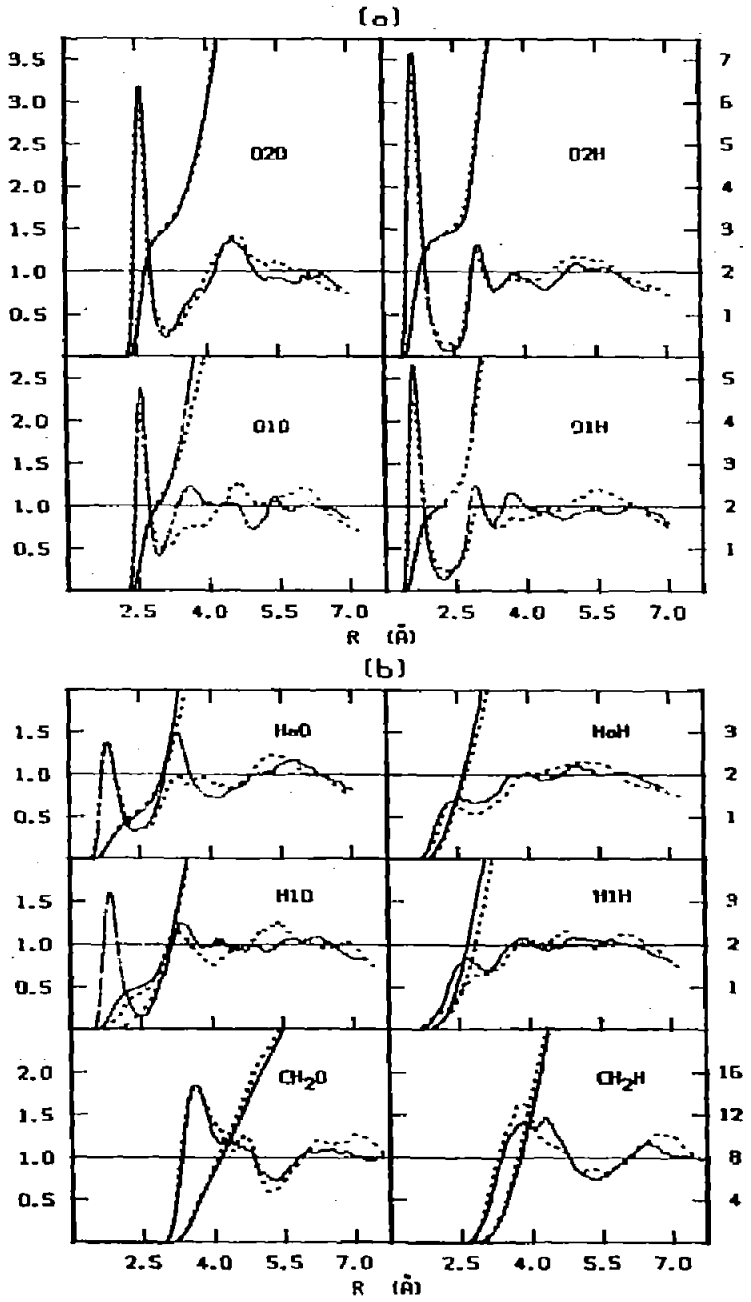

Fig. 2. Radial distribution functions (left scale) and running coordination numbers (right scale) for glycine II (solid line) in comparison with those for glycine I (dashed line): between (a) the solute oxygen atoms, O1 (bottom) and O2 (top), and the water O and Hs, and between (b) the solute CH_2 group (bottom) and hydrogen atoms, H1 (middle), and the average of H2 and H3, Ha (top) and the water O and Hs.

a better evaluation of its effect on the structure of the solution. HaO and HaH are the average radial distribution functions for the other two hydrogens of the NH_3^+ group.

From the examination of these curves it can immediately be seen that:

1) the O2O and O2H rdfs (Fig. 2(a)) are very similar for both glycine conformers (I and II). Also, they closely resemble those recorded in the simulation of the acetate anion. In this solution as well we find strong H-bonds linking O2 to three different water molecules, each of them oriented with one H pointing toward O2, as can be deduced from the coordination numbers and distances of the first peaks of these rdfs.
2) the O1O and O1H rdfs (Fig. 2(a)) are similar for both forms of glycine (at least as far as the first peak is concerned), whereas they differ from those of acetate, that almost coincide with the O2O and O2H rdfs. We explained the height of the first peak of the rdfs for conformer I with the presence of the intra-molecular H-bond preventing the formation of a third H-bond with water. What is the reason of this behaviour? We will discuss this feature in detail later on. For the time being let us pay attention to the subsequent part of the rdfs, which shows the main changes, due to the presence of additional waters in the neighbourhoods. These changes may be ascribed, as will be illustrated below, to the water bound to H1 and to an incoming water unable, however, to reach an H-bond distance in the O1 hydration shell. In their random movement, sometimes, the first shell water molecules may assume slightly unfavoured positions that, conversely, allow enough room to accommodate an additional water molecule.
3) there is no sensitive variation between the CH_2O and CH_2H rdfs in the two solutions (Fig. 2(b)). They are also similar to the CH_3O and CH_3H rdfs obtained for acetate and methylammonium [7].
4) all the three HO and HH rdfs are similar in glycine II, whereas in glycine I only two of them behave in a similar way. As a matter of fact, whilst in glycine II all the three hydrogens of the ammonium group are available

to form (and actually they do) H-bonds with the solvent, in glycine I one of the hydrogens is not available, in that it participate in the intramolecular H-bond. The presence of the third water molecule coordinated to the NH_3^+ group is highlighted, in addition to the value of the running coordination number and to the shape of the first peak in the H1O and H1H rdfs, also by the presence of the second peak in the HaO and H1O rdfs (as well as in the O1O and O1H ones) of glycine II.

Surprisingly, the absence of the intramolecular H-bond is brought out only by the gH1O rdf and the gH1H one, with a hint in the gHaO second maximum, accounting for the water coordinated to the H1 of the NH_3^+ group. The O1O and O1H rdfs, as far as the first maximum and the relevant coordination number are concerned, are practically unaltered. Albeit the O1 atom is available to form one more H-bond, it prefers not (or is not allowed) to. Why? Despite all the analyses performed, we were not able to figure out the reason of this behaviour till we examined a few snapshots (randomly chosen) of the system through our PS330 Evans & Sutherland video display, limiting our observation to the water molecules strongly interacting with the solute. Adding the van der Waals spheres to the solute and solvent molecules it was clear that around such a small solute there is no room left for another water molecule at a correct H-bond distance: a water molecule in turn tried to fill the narrow empty space, but was forced to stay at a much longer distance from the solute. In their random movement, in fact, sometimes the water molecules may assume slightly unfavoured positions allowing enough room to accommodate an additional water molecule.

Cos θ distributions

Further information about the water orientations can be obtained resorting to the cos θ distributions, in which the θ angle is defined as the angle formed by the O-H direction with the X-O axis directed outwards.

The cos θ distributions around the O atoms, reported in Fig. 3, are similar to each other and analogous to those obtained for glycine I, and for acetate and dimethylphosphate [14] as well. They show two equivalent peaks

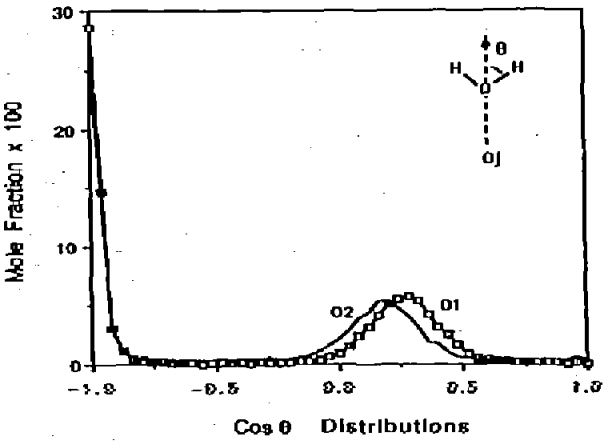

Fig. 3. Cos θ distributions for the waters belonging to the polar O region, O1 and O2. θ angle defined as depicted. Units for the ordinate are mole fraction/0.04 cos θ.

about 180° and 75.5°, in agreement with the HOH angle for water (104.5°), in that each water points one of its hydrogens towards one of the solute oxygens, consistently with what remarked from the running coordination number and from the distance of the first peak in the relevant rdfs. Since these distributions are normalized it is impossible to evaluate the coordination number, that is to be deduced from Fig. 2 and from other analyses. In fact, in this simulation we obtain a coordination number about oxygens of 5.2, that derives from the summation of two different contributions from each oxygen: ~3 from O2 and ~2 from O1. The average coordination numbers in the first hydration shell for this simulation and the related ones are reported in Fig. 4.

The cos θ distributions around the three hydrogens, displayed in Fig. 5, present only one wide maximum about 0.5 (60°), corresponding to water arrangements in which both hydrogens form 60° with the outward normal and therefore the oxygen has both lone pairs pointing towards one of the solute hydrogens. This is a common arrangement obtained also in other systems with the "supermolecule" approach [15]. In the simulation of gly-

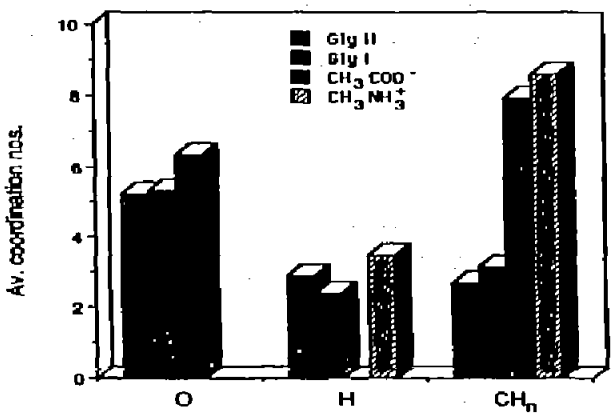

Fig. 4. Comparison of the average coordination numbers for the solute O, H and CH_2/CH_3 groups in the glycine II, glycine I, acetate and methylammonium solutions.

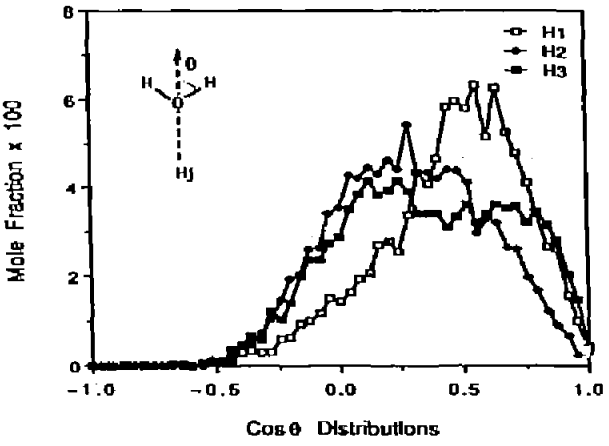

Fig. 5. Cos θ distributions for the waters belonging to the polar H region, H1, H2 and H3. θ angle defined as depicted. Units for the ordinate are mole fraction/0.04 cos θ.

cine I it was possible to draw these distributions for just two hydrogens in an overall agreement with those displayed here. The average coordination numbers with respect to the NH_3^+ hydrogens, also reported in Fig. 4, show that a water molecule is associated with each H. In the other simulations

considered (glycine I and methylammonium) a number somewhat greater than 1 was found for the available Hs since, as already stressed, there is the tendency of a water molecule to fill the empty space coming thus close enough to make an H-bond with the solute molecule.

The hydrophobicity of the CH_2 group is highlighted by the cos θ distributions around it (Fig. 6): the water molecules are generally oriented in such a way as neither hydrogens nor O lone pairs point towards the methylene group. In the previous simulation on glycine I [5] it was possible to observe a slight orientational preference of the water molecules, in that they had both lone pairs pointing toward the CH_2 group, perhaps due to the effort of housing a larger number of water molecules in the first hydration shell. The average coordination numbers (Fig. 4) do not fully account for this effort, since we used a somewhat strict geometrical definition of the first hydration shell in order to avoid the inclusion of second shell waters. An intermediate choice allowing us to discriminate number and position of these incoming waters would have revealed a strong orienting effect of the polar groups also with respect to the water molecules near the border

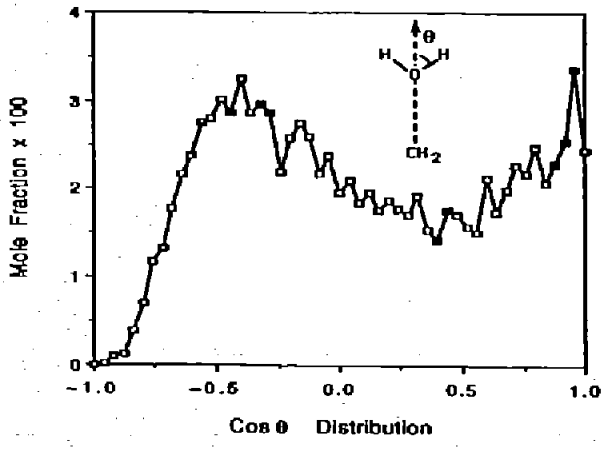

Fig. 6. Cos θ distributions for the waters belonging to the CH_2 region. θ angle defined as depicted. Units for the ordinate are mole fraction/0.04 cos θ.

between the two regions. Notice the large apolar coordination numbers for acetate and methylammonium, whose methyl groups are fully exposed to the solvent.

Additional information can be derived examining the probability of the various polar coordination numbers (Fig. 7, 8). As far as the polar O are concerned, their behaviour is similar in the three solutions even

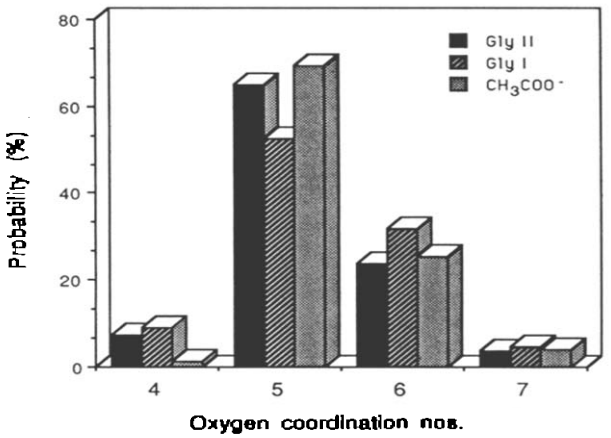

Fig. 7. Probability of various O coordination numbers in the glycine II, glycine I and acetate solutions.

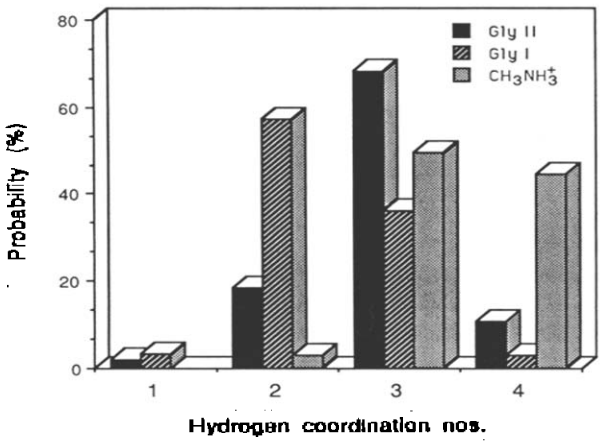

Fig. 8. Probability of various H coordination numbers in the glycine II, glycine I and methylammonium solutions.

though glycine I shows a somewhat larger probability of coordination numbers of 4, 6 and 7 with respect to the other two solutions. The behaviour in the polar H zone is considerably different, since in glycine I there is a higher probability of a coordination number of 2, in glycine II the most probable coordination number is 3, whereas for methylammonium there is an almost equal probability of coordination numbers of 3 and 4.

Differential distance distributions

Another distribution giving a considerable contribution to the knowledge of the reciprocal positions of waters in the various regions is the distribution of the differences between the distances from two different sites. From the $D_{O1\text{-}O2} = |R_{O1W} - R_{O2W}|$ distributions (Fig. 9), as already observed in the COO^- [7] and POO^- [14] groups, it turns out that very few waters are bridged between the two solute oxygens, since they are preferably H-bonded to one oxygen only (Scheme 1). On the contrary from the $D_{Hj\text{-}Hk} = |R_{HjW} - R_{HkW}|$ distributions (Fig. 10), each water associated to one of the hydrogens is seen by the other two hydrogens as bridged between them (Scheme 2): this disposition is the statistically most represented in this

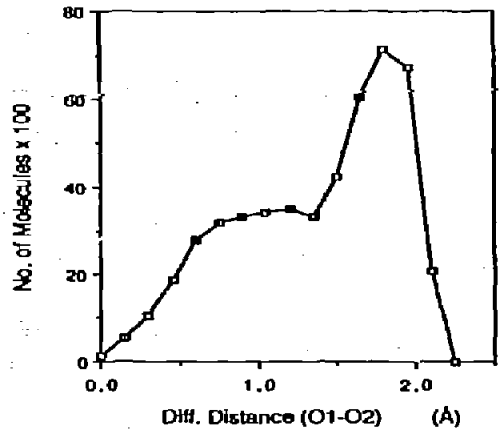

Fig. 9. Differential O1-O2 distance distribution for the water molecules belonging to the polar O region. Units for the ordinate are no. of molecules/0.15 Å.

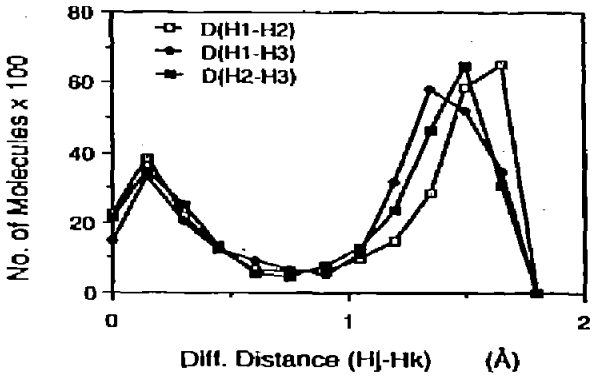

Fig. 10. Differential Hj-Hk distance distributions for the water molecules belonging to the polar H region. Units for the ordinate are no. of molecules/0.15 Å.

region, as can be derived from the small fraction of molecules placed at intermediate differential distances. The situation in this case is completely different from that found in glycine I [5] where, since H1 did not coordinate any water, the D_{H2-H3} distribution presented a sharp peak about 1.5 Å, and the D_{H1-H2} and D_{H1-H3} distributions had a similar trend, showing two equivalent maxima about 0 and 1.5 Å.

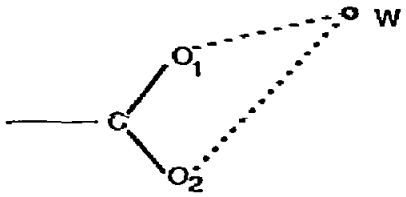

Scheme 1

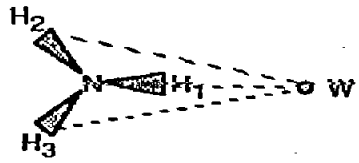

Scheme 2

The arrangement reported in Scheme 2 is the most stable also for the monohydration in the "supermolecule" approach at the ab initio level [16]. Notice that the AM1 results are substantially different, in that they give the bifurcated arrangement as the most stable one [17].

Energetics of the solution

Let us summarize the properties that can be derived from the Monte Carlo simulation.

The total potential energy of the solution can be viewed as the sum of two distinct contributions, due one to solute-solvent interactions and the other to solvent-solvent interactions:

$$E = \overline{E}_{SX} + E_{SS}$$

which are pairwise additive and can be written as:

$$\overline{E}_{SX} = \sum_{i=1}^{N} E_{S_iX} \qquad \text{and} \qquad E_{SS} = \sum_{i=1}^{N} \sum_{j>i}^{N} E_{S_iS_j}$$

The energy of solution (or partial molar internal energy) can be computed if the total energy E°_{SS} of an equal amount of water molecules in the pure liquid is known:

$$\Delta\overline{E}_{sol} = \overline{E}_{SX} + E_{SS} - E^{\circ}_{SS} = \overline{E}_{SX} + \Delta\overline{E}_{SS}$$

The last term $\Delta\overline{E}_{SS}$ can be considered as the solvent disruption due to the presence of the solute.

Subtracting from the volume of the dilute solution, V, that of an equal number of water molecules in the pure liquid, V°, we obtain the partial molar volume of the solution (all the partial molar quantities are indicated by the bar):

$$\Delta\overline{V}_{sol} = V - V^{\circ}$$

From the aforementioned quantities ΔE_{sol} and ΔV_{sol} it is possible to calculate the enthalpy of solution ΔH_{sol}:

$$\Delta\overline{H}_{sol} = \Delta\overline{E}_{sol} + P\Delta\overline{V}_{sol} - RT$$

where RT is the PV contribution for the solute in the ideal gas. In our conditions (1 atm) $\Delta\overline{H}_{sol} \approx \Delta\overline{E}_{sol} - RT$.

The values of the calculated properties are reported in Table 2, together with the results obtained for glycine I [5] in order to facilitate the comparison. The energetics of the solution process is more favourable for glycine II than for glycine I by 2.6 kcal/mol. This overall stabilization comes out from slightly better solute-solvent and solvent-solvent interactions (1.66 and 0.95 kcal/mol, respectively). One could argue that this small energy difference is not sufficient to discriminate absolutely and positively between the two forms, since it does not exclude the presence in solution of

Table 2. Calculated properties for glycine II and glycine I at 25°C and 1 atm[a].

Property[b]	Glycine II	Glycine I
$\overline{E}$	-2254.12 ± 2.0	-2251.51 ± 1.6
$\overline{E}_{SX}$	-115.05 ± 0.5	-113.39 ± 0.8
E_{SS}	-2139.07 ± 2.1	-2138.12 ± 1.8
$\Delta\overline{E}_{SS}$	43.13 ± 4.0	44.08 ± 3.8
$\Delta\overline{E}_{sol}$	-71.9 ± 4.0	-69.3 ± 3.8
V	6653.26 ± 6.2	6529.77 ± 6.8
$\Delta\overline{V}_{sol}$	125.42 ± 18.4	51.05 ± 18.5
$\Delta\overline{H}_{sol}$	-72.4 ± 4	-69.8 ± 4
ρ	0.989	1.0073

[a] Units: energies in kcal·mol^{-1}; volumes in Å^3; ΔV in cm^3·mol^{-1}; ρ in g·cm^{-3}; the standard deviations of the difference quantities are calculated as square root of the sum of the component variances.

[b] TIP4P values for pure water (Ref. 18): E°_{SS} = -2182.2 ± 3.4, V° = 6445 ± 30, ρ°=1.

the H-bonded form. In this case the thermal averaging should be considered, together with the different entropy of the cyclic and distorted forms. The in vacuo thermal contributions to the free energy of the two conformers were thus computed, using the 6-31G* basis set, with *Gaussian 86* [19] that makes use of conventional standard techniques in the harmonic approximation. Their values at the 6-31G* optimized geometries, reported in Table 3 together with the SCF energy and the zero point (ZPE) vibrational term, show that in vacuo glycine I is more stable than glycine II by 5.10 kcal/mol (1.61 kcal/mol in the geometries employed in the Monte Carlo simulations, that are not as much sensitive to a small change in the internal geometries). This result reverses the total energy difference to 2.5 kcal/mol, which value now favours glycine I. The comparison should, of course, be made with the values of the thermal quantities in solution, even though in the case of two stable conformers their differential effect does not considerably change with the dielectric constant of the medium [20].

The solute-solvent energy distribution is displayed in Fig. 11 together

Table 3. Total SCF energy, thermal contributions and zero point energy for glycine II and glycine I (kcal/mol) at 25°C and 1 atm (6-31G* optimized geometries[a]).

	SCF	trasl	rot	vib	therm	ZPE
Glycine II	-282.781089[b]	0.889	0.889	56.160	57.937	55.106
Glycine I	-282.786054[b]	0.889	0.889	55.337	57.115	53.948
Δ(II-I)	3.116	0	0	0.823	0.822	1.158

[a] geometric parameters of glycine II (for the atom numbering see Fig. 1): CO1=1.235 Å, CO2=1.208 Å CC=1.570 Å, CN=1.508 Å, NH2=1.007 Å, NH1,3=1.009 Å, CH=1.080 Å, <OCO=134.42°, <O2CC=113.99°, NCC=105.98°, <H2NC=115.26°, <H1,3NC=107.65°, <H2NH1,3= 111.16°, <H1NH3=103.18°, NCH=108.14°, HCH= 109.91°, HCC=112.22°; geometric parameters of glycine I (H1 is the atom making the intramolecular H-bond): CO1=1.248 Å, CO2=1.203 Å CC=1.569 Å, CN=1.501 Å, NH1=1.076 Å, NH2,3=1.005 Å, CH=1.079 Å, <OCO=133.15°, <O2CC=115.61°, NCC=104.57°, <H1NC=96.53°, <H2,3NC=114.28°, <H1NH2,3= 111.25°, <H2NH3=108.82°, NCH=109.94°, HCH= 109.54°, HCC=111.38°;

[b] Hartrees. (The corresponding 6-31G*/SCF values for the geometries of glycine II and glycine I employed in the Monte Carlo simulations (Table 1) are -282.766691 and -282.769249 hartrees, respectively; ΔE=1.606 kcal/mol)

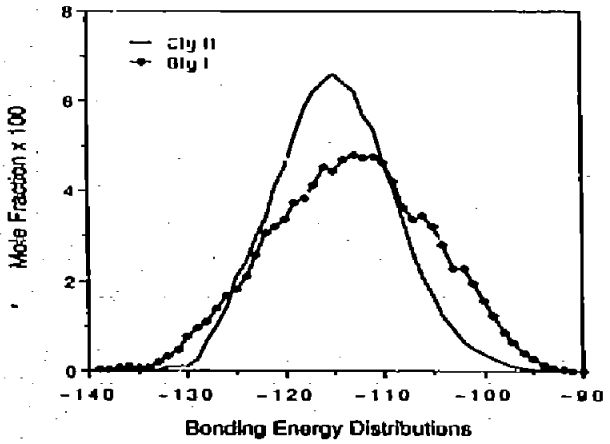

Fig. 11. Solute-water energy distribution for glycine II with respect to glycine I. Units for the ordinate are mole fraction$\times$100 / kcal$\cdot$mol^{-1}.

with the corresponding one for glycine I. On the overall the distribution for glycine II is slightly smoother than for glycine I, as reflected by the values of the corresponding standard deviations. The distribution for glycine II is sharper than that for glycine I, and thus the total solute-solvent energy values show smaller variations along the simulation. Despite the smoother aspect of the solute-solvent energy distribution, the individual solute-solvent interaction energies, reported in Fig. 12, once again in comparison to the glycine I ones, are somewhat less smooth than the latter, even though the overall shape of the two distributions is similar. One feature is brought out by these distributions, namely that the water molecules in the polar regions, where the most attractive contributions are located, prefer to make an additional but less energetic H-bond (thus contributing to increase the volume of the solution) instead of better accommodating a smaller number of water molecules in the first shell.

To analyze the contribution of the various solvation regions (polar O, polar H, apolar) and of the bulk solution to the solute-solvent interaction energy, $\overline{E}_{SX}$, we carried out its decomposition that is reported in Table 4, together with the number of molecules contained in the different regions,

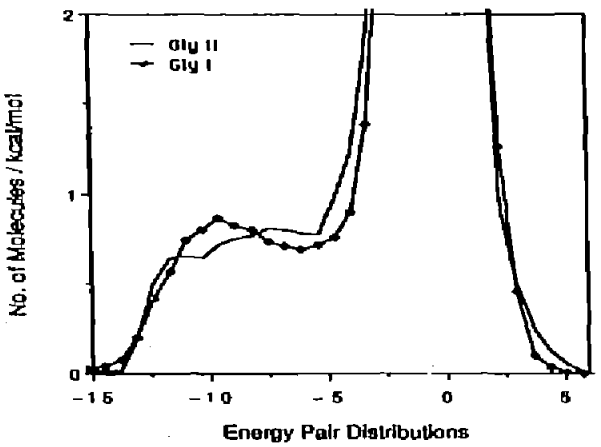

Fig. 12. Solute-water energy pair distribution for glycine II with respect to glycine I.

Table 4. Decomposition of the solvent-solute (S-X) interaction energy in kcal/mol and coordination numbers n within the first solvation shell and the bulk (Fig. 1)[a].

	total values Energy		total values *n*			partial values Energy/*n*	
	Gly II	Gly I	Gly II	Gly I		Gly II	Gly I
PO	-48.4	-51.5	5.2	5.3	O1	-17.3/2.2	-23.3/2.5
					O2	-31.1/3.0	-28.2/2.8
PH	-20.3	-17.0	2.9	2.4	H1	-5.7/0.96	-0.8/0.15
					H2	-7.0/0.87	-8.3/1.11
					H3	-7.6/1.06	-7.9/1.12
A	-5.3	-0.04	2.2	3.1			
Bulk	-41.0	-44.9	205.7	205.2			

[a] Radii employed for the analysis: R(PO) = 3.2 Å, R(PH) = 2.5 Å, R(A) = 4.5 Å.

for glycine II and glycine I [5]. The contributions from water molecules in the polar H and apolar regions are more favourable for glycine II than for glycine I, because there is one more water coordinated to the ammonium group and because of the better geometric arrangement of the hydrophobically bound waters that moreover produces a volume enlargement. On the contrary, the contributions from the waters in the polar O region and in the bulk solution are less favourable than for glycine I: nonetheless, the overall balance favours glycine II. In Table 4, we also report the average solute-solvent energy in each region due to the number of water molecules displayed: the perturbation induced by the effort of housing an additional water molecule in the limited space available in the solute neighbourhoods causes a lengthening of the H-bonds that therefore become less strong, at least as far as the closer groups are concerned (O1 and H1). This is the reason why the additional H-bond does not produce such a large energy gain as might be expected.

A somewhat more difficult discussion is requested to explain the considerable increase in the partial molar volume in passing from I to II,

even though we anticipated some hints. We obtained for I a partial molar volume (51 ± 18 cm^3/mol, [5]) in good agreement with the experimental value (43.3 cm^3/mol, [21]), as was also the case in the simulation of acetate and methylammonium [7]. The calculated sharp increase in the partial molar volume, while all the other computed properties of the solution remain to a certain extent unaltered, seems to be the outstanding feature of this simulation. We may explain it with the larger volume occupied by the first solvation layer, since any sensible choice of the solute van der Waals radii gives substantially equal molecular volumes for the two conformers of the glycine zwitterion. Then this crowded and expanded first layer (just a hint is obtainable from the CH_2H rdf) would cause the water molecules in the second layer to be oriented in an unfavourable way one respect to the other pushing them farther apart in order to reduce the repulsive interaction. The overall balance produces the energetic stabilization at the expenses of the system volume.

As far as the solvent-solvent structural analysis and energetics are concerned, the rdfs are very similar to those recorded for pure water and previously displayed [7], since just a few water molecules belong to the first hydration shell and consequently show a different behaviour with respect to bulk waters, because of the disruption in the pure liquid structure produced by the presence of the solute molecule. An interesting analysis is reported in Fig. 13, 14 which shows the solvent-solvent bonding energy distributions for the water molecules contained in the polar O and H environments in glycine I and II with respect to the same distribution for the water molecules in the bulk solution of glycine II (almost indistinguishable from the energy distribution recorded for pure water). From these distributions the disruption produced in the solvent by the presence of the solute turns out evident and it is quite similar for both polar environments in the same solution.

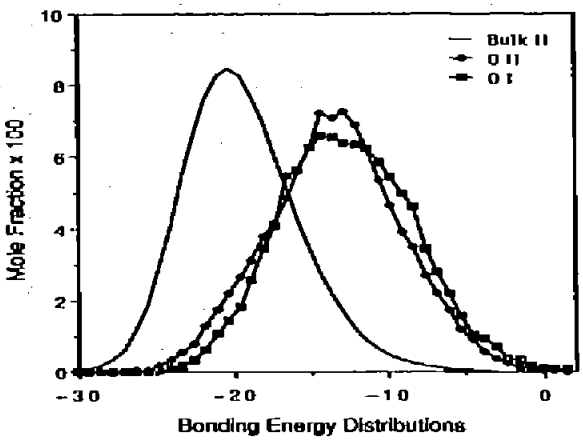

Fig. 13. Solvent-solvent energy distributions as seen by the waters in the polar oxygen environment for glycine II and glycine I, in comparison to the analogous distribution for bulk waters. Units for the ordinate are mole fraction$\times$100 / 0.75 kcal-mol^{-1}.

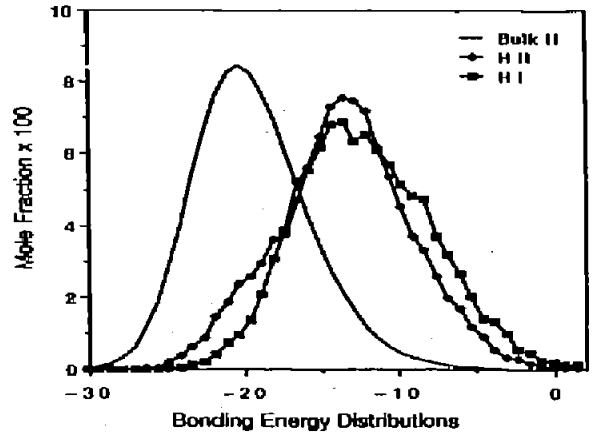

Fig. 14. Solvent-solvent energy distributions as seen by the waters in the polar hydrogen environment for glycine II and glycine I, in comparison to the analogous distribution for bulk waters. Units for the ordinate are mole fraction$\times$100 / 0.75 kcal-mol^{-1}.

Conclusions

The results produced by the Monte Carlo simulation of the glycine zwitterion conformer with a torsional angle of 60° (glycine II) do not

greatly differ from those we have previously obtained [5] for the conformer with a torsional angle of 0° (glycine I), that were already compared to those of previous simulations [8-9] of the glycine I conformer, employing the N,V,T ensemble, different potentials for the solute and solvent molecules and different samples (periodic boundary conditions and a specimen of 215 water molecules or a cluster of 200 water molecules). The solvation energy turns out to be 2.6 kcal/mol more favourable for glycine II than for glycine I, whereas the partial molar volume of solution is exceedingly high for glycine II and in contrast to the experimental value [21], that conversely is well reproduced by the simulation of glycine I. From the energetic results and the above discussion it seems likely that glycine zwitterion prefers the H-bonded form in solution (given also that the isolated glycine I conformer is more favoured by 5.1 kcal/mol, thus reversing the overall energy difference to 2.5 kcal/mol). The small size of the solute, in fact, as well as its limited flexibility prevent the possibility of housing in the first solvation shell a larger number of water molecules. Moreover, the fairly good agreement between the experimental partial molar volume and that computed for glycine I rather supports the presence in solution of the H-bonded form.

References

1. A. Saran, C. K. Mitra, B. Pullman *Biochim. Biophys. Acta*, 517 (1978) 255.
2. A. Saran, *Int. J. Quantum Chem.*, 35 (1989) 193, and refs. quoted therein.
3. G. Alagona, C. Ghio, C. Pratesi *J. Am. Chem. Soc.*, "Force-field Parameters for Dehydroaminoacids" (submitted).
4. O. Pieroni, A. Fissi, S. Salvadori, G. Balboni, R. Tomatis *Int. J. Peptide Protein Res.* 28 (1986) 91.
5. G. Alagona, C. Ghio, P. A. Kollman *J. Mol. Struct. (Theochem)*, 166 (1988) 385.
6. (a) Y.-C. Tse, M. D. Newton, S. Vishveshwara, J. A. Pople *J. Am. Chem. Soc.* 100 (1978) 4329; (b) P. Palla, C. Petrongolo, J. Tomasi *J. Phys Chem.* 84 (1980) 435; (c) R. Bonaccorsi, P. Palla, J. Tomasi *J. Am. Chem. Soc.* 106 (1984) 1945.

7. G. Alagona, C. Ghio, P. A. Kollman *J. Am. Chem. Soc.* 108 (1986) 185.

8. S. Romano, E. Clementi *Int. J. Quantum Chem.* 14 (1978) 839.

9. M. Mezei, P. K. Mehrotra, D. L. Beveridge *J. Biomolec. Struct. and Dynam.* 2(1) (1984) 1.

10. W. L. Jorgensen, J. Chandrasekhar, J. D. Madura, R. W. Impey, M. L. Klein, *J. Chem. Phys.* 79 (1983) 926.

11. U. Chandra Singh, P. A. Kollman *J. Comput. Chem.* 5 (1984) 129.

12. S. J. Weiner, P. A. Kollman, D. A. Case, U. Chandra Singh, C. Ghio, G. Alagona, S. Profeta, Jr., P. Weiner *J. Am. Chem. Soc.* 106 (1984) 765.

13. W. L. Jorgensen *J. Am. Chem. Soc.* 103 (1981) 335.

14. G. Alagona, C. Ghio, P. A. Kollman *J. Am. Chem. Soc.* 107 (1985) 2229.

15. P. Nagy, G. Alagona, C. Ghio, K. Simon, G. Náray-Szabó "Comparative Study of Imidazole Hydration: Ab Initio and Electrostatic Calculations vs. Cambridge Structural Database Analysis", *J. Comput. Chem.* (in press).

16. E. L. Coitiño, K. Irving, J. Rama, O. Ventura XVIII Congreso Internacional de Quimicos Teoricos de Expresion Latina, La Plata (Argentina). Abstracts: p. 42.

17. J. J. Dannenberg, L. K. Vinson *J. Phys. Chem.* 92 (1988) 5635.

18. W. L. Jorgensen, J. Gao *J. Phys. Chem.* 90 (1986) 2174.

19. M. J. Frisch, J. S. Binkley, H. B. Schlegel, K. Raghavachari, C. F. Melius, R. L. Martin, J. J. P. Stewart, F. W. Bobrowicz, C. M. Rohlfing, L. R. Kahn, D. J. DeFrees, R. Seeger, R. A. Whiteside, D. J. Fox, E. M. Fleuder, J. A. Pople, Carnegie-Mellon Quantum Chemistry Publishing Unit, Pittsburgh PA, 1984.

20. G. Alagona, C. Ghio, J. Igual, J. Tomasi *J. Mol. Struct. (Theochem)*, "An Appraisal of Solvation Effects on Chemical Functional Groups: the Amidic and Esteric Linkages" (in press).

21. (a) S. Cabani, G. Conti, E. Matteoli, M. R. Tiné *J. Chem. Soc., Faraday Trans. I*, 77 (1981) 2377; (b) L. Lepori, V. Mollica *Zeitschrift fuer Physikalische Chemie Neue Folge Bd.* 123, S. (1980) 51.